

On the Role of Non-Terrestrial Networks for Boosting Terrestrial Network Performance in Dynamic Traffic Scenarios

Henri Alam^{†‡}, Antonio De Domenico[†], Florian Kaltenberger[‡], David López-Pérez[★]

[†]Huawei Technologies, Paris Research Center, 20 quai du Point du Jour, Boulogne Billancourt, France.

[‡]EURECOM, 2229 route des Crêtes, 06904 Sophia Antipolis Cedex, France.

[★]Universitat Politècnica de València, Spain.

Abstract—Due to an ever-expansive network deployment, numerous questions are being raised regarding the energy consumption of the mobile network. Recently, Non-Terrestrial Networks (NTNs) have proven to be a useful, and complementary solution to Terrestrial Networks (TN) to provide ubiquitous coverage. In this paper, we consider an integrated TN-NTN, and study how to maximize its resource usage in a dynamic traffic scenario. We introduce BLASTER, a framework designed to control User Equipment (UE) association, Base Station (BS) transmit power and activation, and bandwidth allocation between the terrestrial and non-terrestrial tiers. Our proposal is able to adapt to fluctuating daily traffic, focusing on reducing power consumption throughout the network during low traffic and distributing the load otherwise. Simulation results show an average daily decrease of total power consumption by 45% compared to a network model following 3GPP recommendation, as well as an average throughput increase of roughly 250%. Our paper underlines the central and dynamic role that the NTN plays in improving key areas of concern for network flexibility.

I. INTRODUCTION

With the swift evolution of cellular communications in recent years, there has been a significant upswing in the demand for high-speed data connectivity. This has led to the imposition of strict prerequisites to deliver high capacity and ensure ubiquitous connectivity for the network. The use of heterogeneous networks (HetNets) has been proposed as a solution to address these requirements [1]. Indeed, the use of HetNets creates a multi-layered network, allowing efficient data offloading which improves both the capacity and the coverage throughout the network. However, this dense deployment increases the overall energy consumption of the network, which is not desirable given the current environmental and economic context. Hence, one of the key objectives of deploying and operating mobile networks is to reduce power usage while ensuring to meet Quality of Service (QoS) requirements [2]. In the past few years, non-terrestrial networks (NTNs) have arisen as a feasible approach to supplement the terrestrial network (TN) and extend coverage to previously underserved geographic regions [3]. An NTN is a network in which airborne vehicles like drones (i.e. unmanned aerial vehicles),

high-altitude platform stations (HAPS), or satellites function as a relay node or base station (BS) to provide connectivity for each user equipment (UE) within the network. The inherent advantage of NTNs lies in their ability to offer extensive coverage across vast regions, including remote geographical areas where deploying terrestrial macro BSs (MBSs) would be cost-prohibitive or logistically challenging. Among the various deployment possibilities, it appears that low-earth orbit (LEO) satellites will lead the way in achieving high-capacity connectivity from space [4]. They orbit at altitudes ranging from 200 to 2000 kilometers. Due to their closer proximity to Earth, they offer superior signal strength and reduced latency when compared to alternative satellite designs. This results in lower energy requirements for launch and decreased power consumption for signal transmission from/to the satellite. Considering all of these factors, integrated TN-NTN may be the path towards efficient service of both terrestrial and aerial UEs [5]. Typically, each UE is connected to the BS with the strongest recorded Reference Signal Received Power (RSRP) within the network. However, this association strategy has its limits as it does not consider the varying traffic demands of UEs, potentially resulting in suboptimal load balancing and subsequent performance issues. An improved UE association policy should not only consider the strength and quality of the UE's signal but also factor in the load on each cell. Our previous work in [6] addresses this specific problem in an integrated TN-NTN. We were able to distribute the network load with the help of satellites and enhance the maximum network throughput as well as improve network coverage. Regarding Energy Efficiency (EE), we acknowledge that utilizing all MBSs during low-traffic scenarios (e.g. night) might not be ideal. Indeed, most of them may be under-utilized or not used at all, resulting in an inefficient allocation of energy and communication resources. Hence, given the context of an integrated TN-NTN, it may be appropriate to turn off part of the terrestrial MBSs and offload the UEs to the satellites to reduce energy consumption. To the extent of our knowledge, most of the work related to BS activation does not consider the NTNs as a solution to the problem of maintaining coverage and capacity requirements while shutting down MBSs. The authors of [7] implement a switching-on/off-based energy-saving algorithm that shuts down the MBSs

This research is supported by the Generalitat Valenciana through the CIDEENT PlaGenT, Grant CIDEXG/2022/17, Project iTENTE, and by the action CNS2023-144333, financed by MCIN/AEI/10.13039/501100011033 and the European Union "NextGenerationEU"/PRTR.

one by one while making sure that they do not overload the neighbouring MBSs. To maintain the user experience, some of the works have considered minimal QoS requirements. In [8], the authors study the impact of traffic offloading in HetNets on energy consumption and suggest a centralized Q-learning approach for achieving a balance between conserving energy and ensuring QoS satisfaction. The authors of [9] develop an algorithm that allows each UE to associate with multiple MBSs on different frequency bands, and optimize the MBS's transmit power simultaneously so that they can be shut down during low traffic.

In this paper, we present a Bandwidth spLit, user ASsociation and PowEr contROl framework (BLASTER). It is a novel adaptive radio resource management framework, which controls the bandwidth split, UE association, terrestrial MBS transmit power and activation in an integrated TN-NTN. It is able to trade-off between network capacity and network energy consumption based on the traffic state. Our results show that the proposed framework reduces the average network power consumption by 45% compared to an integrated TN-NTN model following 3GPP recommendations, while significantly improving the mean throughput during high-traffic periods.

II. SYSTEM MODEL

We study a downlink (DL) cellular network comprising M terrestrial MBSs and N MBSs mounted on LEO satellites, totalling L , all of which can serve K UEs deployed in a rural area. We denote the total system bandwidth as W , which the mobile network operator allocates between the terrestrial and non-terrestrial tiers. In our research, we assume that this network operates in the S band at approximately 2 GHz, with terrestrial and satellite MBSs utilizing orthogonal portions of it. Throughout the remainder of this paper, we will use \mathcal{T} (representing terrestrial) and \mathcal{S} (representing satellites) to denote the sets of MBSs. Furthermore, let $\mathcal{U} = \{1, \dots, i, \dots, K\}$ be the set of UEs and $\mathcal{B} = \mathcal{T} \cup \mathcal{S} = \{1, \dots, j, \dots, L\}$ the set of all MBSs. Concerning the channel model, the large-scale channel gain between a terrestrial MBS j and a UE i is computed as follows:

$$\beta_{ij} = G_{T_x} \cdot PL_{ij} \cdot SF_{ij}, \quad (1)$$

where G_{T_x} is the transmit antenna gain, PL_{ij} is the path loss, and SF_{ij} is the shadow fading. Note that the UE antenna gain is 0 dBi. Conversely, when a satellite MBS j serves a UE i , the large-scale channel gain is the following [10]:

$$\beta_{ij} = G_{T_x} \cdot PL_{ij} \cdot SF_{ij} \cdot CL \cdot PL_s. \quad (2)$$

In (2), CL represents clutter loss, an attenuation due to buildings and vegetation near the UE, while PL_s accounts for scintillation loss, which encompasses rapid fluctuations in signal amplitude and phase caused by ionospheric conditions. Given that each UE is exclusively served by either a terrestrial or a satellite MBS, and both tiers operate without interference due to their orthogonal bandwidth allocation, we can compute

the large-scale Signal-to-Interference-plus-Noise Ratio (SINR) for each UE i as outlined below:

$$\gamma_{ij} = \frac{\beta_{ij} p_j}{\sum_{j' \in \mathcal{I}_j} \beta_{ij'} p_{j'} + \sigma^2}, \quad (3)$$

where p_j is the transmit power allocated per resource element (RE) at MBS j , \mathcal{I}_j represents the set of MBSs causing interference to the serving MBS j , and σ^2 is the noise power per RE. Subsequently, if we assume that MBS j evenly allocates its available bandwidth W_j among the k_j UEs it serves, we can calculate the average throughput for UE i connected to MBS j as follows:

$$R_{ij} = \frac{W_j}{k_j} \log_2(1 + \gamma_{ij}). \quad (4)$$

The power consumption model for a terrestrial MBS depends on multiple parameters, such as bandwidth, number of antennas, or power amplifier efficiency, as detailed in [11]. This model can be compacted as:

$$Q_j(p_j) = P_0 + p_j + \psi_j \|p_j\|_0, \quad (5)$$

where ψ_j and p_j respectively include all the static (transmit power independent) and dynamic (transmit power dependent) components of the model, and $\|\cdot\|_0$ is a binary-valued function equal to 1 if the transmit power p_j is greater than 0. P_0 is the power consumption of the components that stay active in a shutdown terrestrial MBS. We suppose that the power consumed by a satellite is harvested from solar panels. In the following, please note that we will be referring to the Hadamard product using the symbol \odot .

III. PROBLEM FORMULATION

We aim to design a mechanism that jointly optimizes network capacity and TN energy consumption by dynamically adapting the resource allocation to the network load. By maximizing the sum of the log-throughput (SLT) perceived by each UE, we want to ensure proportional fairness as the nature of the logarithm prevents excessive use of resources for a particular UE, promoting a proportional allocation of resources. We define ε as the portion of the bandwidth allocated for the LEO satellites. Consequently, we can calculate the bandwidth W_j for MBS j as $W\varepsilon$ when it is a satellite, or as $W(1 - \varepsilon)$ when it is a terrestrial MBS. Let us also introduce a binary variable, denoted as x_{ij} , which takes the value of 1 when UE i is connected to MBS j and 0 otherwise. We can then write the perceived throughput for UE i as:

$$R_i = \sum_{j \in \mathcal{B}} x_{ij} R_{ij}. \quad (6)$$

Our target is to optimize the UE-BS association, the transmit power at each MBS, and the allocation of bandwidth to each tier to find the right trade-off between maximizing the network SLT and minimizing the terrestrial network power

consumption, by shutting down as many terrestrial MBSs as possible. This can be written as follows:

$$\max_{X, \varepsilon, p} \sum_{i \in \mathcal{U}} \log(R_i) - \lambda \sum_{j \in \mathcal{B}} Q_j(p_j) \quad (7a)$$

$$\text{s.t.} \quad x_{ij} \in \{0, 1\}, \quad i \in \mathcal{U}, j \in \mathcal{B}, \quad (7b)$$

$$\tilde{\beta} \cdot p \geq RSRP_{\min} \cdot \mathbb{1}_K, \quad \forall i \in \mathcal{U}, \quad (7c)$$

$$p_j \leq p_j^{\text{MAX}}, \quad \forall j \in \mathcal{B}, \quad (7d)$$

$$\varepsilon \in [0, 1], \quad (7e)$$

where $X = [x_{ij}]$ is the binary association matrix, $p = [p_1, \dots, p_L]^T$ is the vector representing the transmit power at each MBS and $\tilde{\beta} = X \odot \beta$. Also, λ is a scaling parameter used to manage the trade-off between SLT and power consumption, and fixed prior to the optimization, accordingly to the expected user traffic. Constraint (7c) guarantees that the minimum RSRP for each UE must exceed a predefined threshold $RSRP_{\min}$. Additionally, constraint (7d) limits the maximum transmit power allocated per RE in each MBS j to p_j^{MAX} . Since one of our aims is to reduce the terrestrial network power consumption, a sparse solution for the power vector p would be ideal. However, since the power consumption model (5) contains a non-continuous term, it may be hard to optimize. With this in mind, we approximate the utility function (7a) by introducing a mixed L_1 - L_2 penalty function which promotes group sparsity, as done in [12]. We then have the following:

$$\max_{X, \varepsilon, p} \sum_{i \in \mathcal{U}} \log(R_i) - \lambda \left(\|p\|_1 + \sum_{j=1}^L \psi_j w_j \|p\|_2 \right) \quad (8a)$$

$$\text{s.t.} \quad (7b) - (7e), \quad (8b)$$

where $\|\cdot\|_1$, $\|\cdot\|_2$ represent the L_1 and L_2 norm and w_j represents the power weight of MBS j . Those weights are inversely proportional to the transmit power of each MBS, hence pushing those with low transmit power to be shut down.

IV. FULL BREAKDOWN OF BLASTER

In this section, we study BLASTER, the framework proposed to solve the optimization problem (8a)-(8b). We use the block coordinate gradient ascent (BCGA) algorithm, meaning that we first optimize the UE-BS association and bandwidth allocation considering fixed transmit power, similarly to [6]. Thereafter, we optimize the transmit power level considering the first two parameters fixed.

A. Utility optimization under fixed transmit power

Denoting by f the utility function that we want to maximize in (8a), we notice that we have a convex optimization problem with respect to X (ε and p being fixed). We can then use the iterative gradient projection method to solve the problem, as it is particularly well-suited for constrained optimization problems. It consists of computing the gradient and projecting

it onto the feasible region defined by the constraints. Embracing the gradient projection method, we compute the gradient update at time-step s as:

$$\tilde{X}(s) = X(s) + \alpha \nabla_X f(X, p, \varepsilon), \quad (9)$$

where $\alpha \in \mathbb{R}^{K \times L}$ is a step-size chosen appropriately and ∇ is the gradient operator. Then, we write the projection step in the following form:

$$\min_{X(s)} \frac{1}{2} \|X(s) - \tilde{X}(s)\|_F^2 \quad (10a)$$

$$\text{s.t.} \quad \tilde{\beta} \cdot p \geq RSRP_{\min} \cdot \mathbb{1}_K, \quad (10b)$$

where $\|\cdot\|_F$ represents the Frobenius norm. For the following, we simplify the notation by omitting time-step indices. To solve (10a)-(10b), we use the Lagrange multipliers method. Therefore, we compute the Lagrangian function associated with the problem:

$$\begin{aligned} \mathcal{L}(X, \mu) &= \frac{1}{2} \|X - \tilde{X}\|_F^2 + \left(\tilde{\beta} \cdot p - RSRP_{\min} \cdot \mathbb{1}_K \right)^T \mu \\ &= \frac{1}{2} \|X\|_F^2 - \text{Tr}(X^T \tilde{X}) + \frac{1}{2} \|\tilde{X}\|_F^2 + \left(\tilde{\beta} \cdot p \right)^T \mu \\ &\quad - (RSRP_{\min} \cdot \mathbb{1}_K)^T \mu, \end{aligned} \quad (11)$$

where $\mu \in \mathbb{R}^K$ is the Lagrange multiplier associated with constraint (7c). Computing the gradient of (11) with respect to X , we get:

$$\nabla_X \mathcal{L}(X, \mu) = X - \tilde{X} + \beta \odot \underbrace{(\mathbb{1}_K \cdot p^T)}_{:=p^{\text{PAD}}} \odot \underbrace{(\mu \cdot \mathbb{1}_L^T)}_{:=\mu^{\text{PAD}}}. \quad (12)$$

Then, we know that the optimal value to minimize (11) with a fixed dual variable is:

$$X^* = \max\{\tilde{X} - \beta \odot p^{\text{PAD}} \odot \mu^{\text{PAD}}, 0\}. \quad (13)$$

Having computed X^* , we thereby introduce the Lagrangian dual function, which can be written as:

$$\mathcal{D}(\mu) = \max_X \mathcal{L}(X, \mu). \quad (14)$$

Hence, after injecting (13) into the formula above, we get:

$$\begin{aligned} \mathcal{D}(\mu) &= \mathcal{L}(X^*, \mu) \\ &= \frac{1}{2} \|X^*\|_F^2 - \text{Tr}(X^{*T} \tilde{X}) + \frac{1}{2} \|\tilde{X}\|_F^2 \\ &\quad + \left[(X^* \odot \beta) \cdot p \right]^T \mu - (RSRP_{\min} \cdot \mathbb{1}_K)^T \mu. \end{aligned} \quad (15)$$

By noticing that

$$\left[(X^* \odot \beta) \cdot p \right]^T \mu = \text{Tr} \left(X^* \left(\beta \odot p^{\text{PAD}} \odot \mu^{\text{PAD}} \right)^T \right),$$

we can rewrite (15) as:

$$\begin{aligned} \mathcal{D}(\mu) &= \frac{1}{2} \|X^*\|_F^2 - \text{Tr} \left(X^* \left[\tilde{X} - \beta \odot p^{\text{PAD}} \odot \mu^{\text{PAD}} \right]^T \right) \\ &\quad - (RSRP_{\min} \cdot \mathbb{1}_K)^T \mu. \end{aligned} \quad (16)$$

Also, as the authors of [9] demonstrated, we know that

$$\frac{1}{2} \left\| \max\{A, 0\} \right\|_F^2 - \text{Tr}(\max\{A, 0\}A^T) = -\frac{1}{2} \left\| \max\{A, 0\} \right\|_F^2$$

for a given matrix A .

Therefore, we can write the dual problem associated with (10a) as the following:

$$\min_{\mu} \frac{1}{2} \|X^*\|_F^2 + (RSRP_{\min} \cdot \mathbb{1}_K)^T \mu \quad (17a)$$

$$\text{s.t.} \quad \mu \leq 0 \quad (17b)$$

Since this problem has a sole constraint, and we know that the projection onto the non-positive orthant is a straightforward task, we can use the gradient projection method to solve it. After obtaining the solution to the problem above, we obtain μ^* and can retrieve the optimal solution to our projection problem (10a)-(10b):

$$X(s+1) \triangleq X^* = \max\{\tilde{X}(s) - \beta \odot p^{\text{PAD}} \odot \mu^{*\text{PAD}}, 0\}. \quad (18)$$

After the convergence of this method, we are able to find the optimal association X^* . Afterwards, we need to split the bandwidth between both tiers in an optimal way. To drive the process, we introduce r_{ij} as:

$$r_{ij} = \frac{W}{k_j} \log_2(1 + \gamma_{ij})$$

such that:

$$R_{ij} = \begin{cases} \varepsilon r_{ij} & \text{if } j \in \mathcal{S}, \\ (1 - \varepsilon) r_{ij} & \text{otherwise.} \end{cases} \quad (19)$$

As both the transmit power allocated by the cells and the noise power linearly increase with the bandwidth, γ_{ij} does not depend on it. Therefore, we can compute the gradient of our utility function f with respect to ε :

$$\begin{aligned} \nabla_{\varepsilon} f(X, p, \varepsilon) &= \frac{\partial}{\partial \varepsilon} \left(\sum_{i=1}^K \log(R_i) \right) = \sum_{i=1}^K \frac{\partial}{\partial \varepsilon} \log(R_i) \\ &= \sum_{i=1}^K \frac{\sum_{j \in \mathcal{S}} \frac{\partial}{\partial \varepsilon} [\varepsilon x_{ij} r_{ij}] + \sum_{j \in \mathcal{T}} \frac{\partial}{\partial \varepsilon} [(1 - \varepsilon) x_{ij} r_{ij}]}{R_i} \\ \Leftrightarrow \nabla_{\varepsilon} f(X, p, \varepsilon) &= \sum_{i=1}^K \left[\frac{\sum_{j \in \mathcal{S}} x_{ij} r_{ij} - \sum_{j \in \mathcal{T}} x_{ij} r_{ij}}{R_i} \right] \end{aligned} \quad (20)$$

By noticing that $\mathcal{U} = \mathcal{U}_{\mathcal{S}} \cup \mathcal{U}_{\mathcal{T}}$, where $\mathcal{U}_{\mathcal{S}}$ and $\mathcal{U}_{\mathcal{T}}$ represent the set of UEs served by the satellites and terrestrial MBSs respectively, we are able to find the optimal split by forcing (20) to 0:

$$\begin{aligned} \nabla_{\varepsilon} f(X, p, \varepsilon) = 0 &\Leftrightarrow \sum_{i \in \mathcal{U}_{\mathcal{S}}} \frac{1}{\varepsilon} + \sum_{i \in \mathcal{U}_{\mathcal{T}}} \frac{-1}{1 - \varepsilon} = 0 \\ \Leftrightarrow \frac{K_{\mathcal{S}}}{\varepsilon} - \frac{K - K_{\mathcal{S}}}{1 - \varepsilon} = 0 &\Leftrightarrow \varepsilon^* = \frac{K_{\mathcal{S}}}{K} \end{aligned} \quad (21)$$

where $K_{\mathcal{S}}$ represents the number of UEs associated to a

satellite in the network. From eq. (21), we notice that the share of allocated bandwidth for the non-terrestrial tier correlates intuitively with the number of UEs associated to a satellite.

B. Transmit power optimization under fixed association

After addressing the UE-BS association and bandwidth allocation challenges, we fix X and ε to fine-tune the transmit power at each terrestrial MBS and ultimately, maximize the utility function. The transmit power optimization problem can then be expressed as:

$$\max_p \sum_{i \in \mathcal{U}} \log(R_i) - \lambda \left(\|p\|_1 + \sum_{j=1}^L \psi_j w_j \|p\|_2 \right) \quad (22a)$$

$$\text{s.t.} \quad (7c) - (7d) \quad (22b)$$

Due to the non-smoothness of the L_1 norm, we have to resort to the iterative proximal gradient method [13] to solve (22a)-(22b). The gradient update at time-step s is computed as such:

$$\tilde{p}(s) = p(s) + \eta \nabla_p f(X, p, \varepsilon) \quad (23)$$

where $\eta \in \mathbb{R}^L$ is a step-size chosen appropriately. As demonstrated in [13], the proximal gradient method updates p by solving the following problem:

$$\min_p \frac{1}{2} \|\tilde{p}(s) - p(s)\|_2^2 + t \|p(s)\|_2 \quad (24a)$$

where

$$t = \lambda \cdot \eta \cdot w^T \psi. \quad (25)$$

This problem has a closed-form solution, referred to as block soft thresholding [13, Sec. 6.5.1]:

$$\hat{p}(s) = \max\left\{1 - \frac{t}{\|\tilde{p}(s)\|_2}, 0\right\} \tilde{p}(s). \quad (26)$$

Once we have updated the transmit power vector, we must project it into a feasibility region which would ensure that constraints (7c) and (7d) are respected.

Naturally, the upper bound of our feasible region is the maximum transmit power per RE. To establish the lower limit, we use the minimal coverage constraint. In fact, from (7c) we know that each UE associated with a MBS j should experience a signal power level exceeding the threshold value of $RSRP_{\min}$. This can be rewritten as:

$$\forall i \in \mathcal{U}_j, \quad p_j \geq \frac{RSRP_{\min}}{\beta_{ij}}, \quad (27)$$

with \mathcal{U}_j being the set of UEs associated to the MBS j . We are therefore able to establish the lower bound of the feasibility region for each MBS j as:

$$\tau_j = \max_{i \in \mathcal{U}_j} \left(\frac{RSRP_{\min}}{\beta_{ij}} \right). \quad (28)$$

Finally, the transmit power update done at the end of step s is written as such:

$$p(s+1) = \left[\hat{p}(s) \right]_{\tau_j}^{p^{\text{MAX}}}. \quad (29)$$

Once the algorithm has converged and we obtain p^* , we

update the power weights w_j according to the re-weighting algorithm detailed in [9]. The full optimization framework is summarized below in Algorithm 1.

Algorithm 1: BLASTER Framework

Data: K UEs and L MBs.
Initialization;
 $s = 0$;
X: Association done through max-RSRP;
p: Transmit power set to maximum;
 $\varepsilon = 0.5$; // Equal bandwidth split
Compute: $f(X, \varepsilon, p)$ // Initial point
 $w = [1, \dots, 1] \in \mathbb{R}^L$;
Initialize $\alpha \in \mathbb{R}^{K \times L}$, $\mu \in \mathbb{R}^K$;
Initialize $\eta \in \mathbb{R}^L$;
while Utility function f has not converged **do**
// UE Association and bandwidth split
Compute: $\tilde{X}(s) = X(s) + \alpha \nabla_X f(X, p, \varepsilon)$ (9);
Solve (17a) using gradient projection to obtain μ^* ;
Compute:
 $X(s+1) = \max\{\tilde{X}(s) - \beta \odot p^{\text{PAD}} \odot \mu^{*\text{PAD}}, 0\}$ (18);
 $\varepsilon^* = \frac{Ks}{K}$ (21);
// Power control step
Compute: $\tilde{p}(s) = p(s) + \eta \nabla_p f(X, p, \varepsilon)$ (23);
Compute: $t = \lambda \cdot \eta \cdot w^T \psi$ (25);
Compute: $\hat{p}(s) = \max\{1 - \frac{t}{\|\tilde{p}(s)\|_2}, 0\} \tilde{p}(s)$ (26);
Compute: τ based on (28);
Compute: $p(s+1) = \left[\hat{p}(s) \right]_{\tau}^{p^{\text{MAX}}}$ (29);
 $w = \left[\frac{1}{p_1 + \delta}, \dots, \frac{1}{p_L + \delta} \right]$;
// δ small constant to avoid numerical instability
Compute: $f(X(s), \varepsilon, p(s))$;
 $s = s + 1$;
end
return X, ε, p ;

V. SIMULATION RESULTS AND ANALYSIS

In this section, we evaluate the performance of our framework within the context of an integrated TN-NTN for a duration of 24 hours, with a varying number of UEs at each hour, as illustrated in [14]. We consider a rural scenario where the terrestrial MBSs are deployed in a hexagonal grid pattern [15]. We focus our study on an area of roughly 2500 km², which corresponds to the coverage range of an LEO satellite beam [16]. Moreover, we assume that the LEO constellation employs earth-fixed beams [10] and that the beam serving our scenario originates from a satellite with a 90 degree elevation angle. All of the UEs are distributed uniformly throughout the grid. We provide two settings as benchmarks: The 3GPP-TN setting in which there is no satellite tier and the terrestrial tier gets a total bandwidth of 10 MHz, and the 3GPP-NTN setting, where the bandwidth is split according to the 3GPP

specifications [16], meaning that 30 MHz is allocated to the satellite tier and 10 MHz to the terrestrial tier. In both settings, the UEs associate with the BSs following the max-RSRP rule and there is no DL transmit power optimization or MBS shutdown. Note that λ is set such that it is inversely proportional to the number of UEs in the network. Most of the relevant simulation parameters can be found in Table I, set accordingly to [10], [16]–[20].

Parameter	Value
Total Bandwidth W	40 MHz
Carrier frequency f_c	2 GHz
Subcarrier Spacing	15 kHz
Urban/Rural Inter-Site Distance	500/1732 m
Number of Macro BSs	1067
Satellite Altitude [16]	600 km
Terrestrial Max Tx Power per RE p_j^{MAX} [19]	17.7 dBm
Satellite Max Tx Power per RE p_j^{MAX} [16]	15.8 dBm
Antenna gain (Terrestrial) G_{T_X} [20]	14 dBi
Antenna gain (Satellite) G_{T_X} [16]	30 dBi
Shadowing Loss (Terrestrial) SF [18]	4 – 8 dB
Shadowing Loss (Satellite) SF [10]	0 – 12 dB
Line-of-Sight Probability (Satellite / Terrestrial)	Refer to [10] / [18]
White Noise Power Density	−174 dBm/Hz
Coverage threshold $RSRP_{\min}$	−120 dBm

Table I: Simulation parameters.

A. Sum Throughput Analysis

In this section, we analyze the sum throughput of the network, to better understand how our framework adapts the offered capacity to the actual load of the network. In this regard, Fig. 1 shows the evolution of the sum throughput (ST) during an entire day and for different traffic states. On top of the two benchmarks, we plot the hourly ST for 1) BLASTER (presented in Sec. IV) and 2) a setting where the association and power control are based on our algorithm, but bandwidth is shared equally among both tiers (Fixed bandwidth split). Firstly, we notice that although the

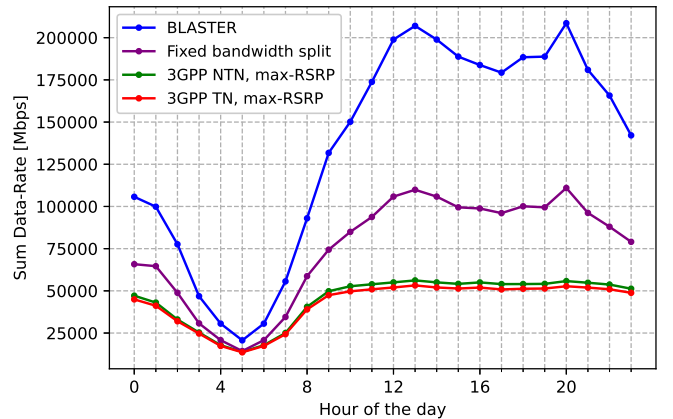


Figure 1: Network Sum Throughput throughout the day for different scenarios.

network ST gain provided by our framework is limited during low and average traffic periods (e.g. early morning), we see a clear improvement during high-traffic hours. This is

explained by the fact that when the traffic load is low, the algorithm favours energy saving since the value of λ has been set to a greater value, to penalize power consumption and drive the terrestrial MBSs to shut down at the expense of the ST. Inversely, when traffic is high, our framework distributes the load and redistributes the bandwidth resources so that the network ST improves notably. Indeed, compared to the 3GPP-NTN benchmark, we see a growth of the sum throughput which can go up to as much as 270% during peak traffic. As expected, the 3GPP-TN setting provides the worst performance amongst the compared solutions. This is due to the fact that, without satellites, roughly 7% of the UEs are out of coverage [6] and the overall available total bandwidth is limited. 3GPP-NTN improves the ST due to the addition of a satellite tier, which provides coverage for the entire grid, as well as a solution for UEs who are associated to overloaded terrestrial MBSs and perceiving a low throughput. Moreover, considering the settings with our power optimization and UE-BS association, we see that the ST further improves. This results from reduced interference from neighbouring terrestrial MBSs due to the power control step, leading to a throughput increase. Furthermore, we notice that the dynamic allocation of the bandwidth benefits the network ST, as we can see it double compared to Fixed Bandwidth split during high traffic. Finally, we observe an average increase of 249% in terms of mean throughput during high traffic compared to 3GPP-NTN, which underlines the effectiveness of our framework.

B. Satellite Offloading Analysis

In this section, we study the critical role that the satellite plays in our framework by analyzing the proportion (see Fig. 2) of UEs associated to a satellite throughout the day.

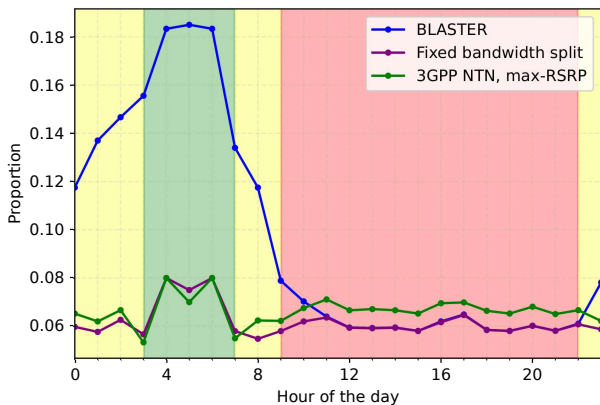


Figure 2: Proportion of UEs associated to the satellite throughout the day.

The load of the traffic is represented by the background colour, i.e. green, yellow, and red are low, average, and high-traffic hours respectively. We know that during low traffic, the onus is on reducing the TN power consumption. Therefore, the satellite becomes an attractive means to serve UEs. Thanks to our method, this results in an increased proportion (more than a 200% increase) of UEs associated to a satellite compared

to the benchmark 3GPP-NTN. As a result, we are able to shut down more terrestrial MBSs during low-traffic hours. On the contrary, we see that the satellite associates with fewer UEs during high-traffic hours. Indeed, the proportion of UEs associated to it is lesser than in the 3GPP-NTN scenario. This can be explained by the fact that when the traffic is high, the satellite will act more as a coverage layer. Most of the satellite bandwidth is allocated to the terrestrial MBSs, as the TN can support higher throughputs due to the large spectrum reuse. Therefore, we notice how the algorithm is able to adapt the overall TN-NTN resources according to traffic variations.

C. Power Consumption Analysis

In this section, we investigate the performance of our framework in terms of power consumption. As mentioned above, terrestrial MBSs transmit power and activation control plays an important role in our proposed framework. In Fig. 3, we show the network power consumption throughout the day for the various solutions analyzed in this paper. The

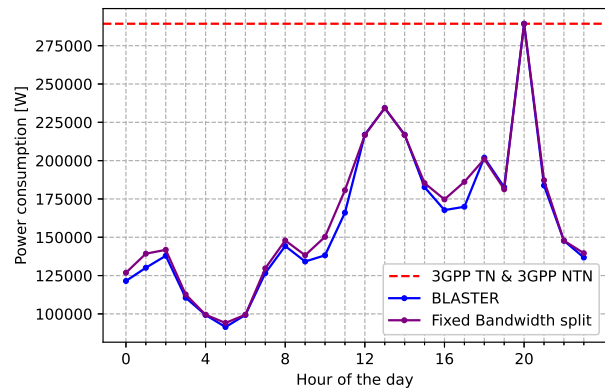


Figure 3: Network Power consumption throughout the day.

dotted red line represents the power consumption level for both 3GPP benchmarks. As explained before, since there is no power optimization or terrestrial MBS shutdown in those settings, the transmit power levels are at the maximum throughout the day. We observe an average decrease of the network power consumption by 65.4% during low traffic for our framework, compared to both 3GPP benchmarks. This is because, as we discussed in Sec. V-B, the satellites take a prominent role at this period of the day, associating with more UEs than in the 3GPP-NTN network setting. This allows the shutdown of many terrestrial MBSs and saves a lot of energy in the process. Also, during high traffic, we notice that the average network power consumption decreases by 33%. As the shutdown of MBSs is not the priority during this period, the energy saved is mostly due to some BSs decreasing their transmit power without negatively impacting the QoS. The noticeable improvement in ST observed in Fig. 1 during high traffic corroborates this statement. Once again, this highlights the ability of our network to adapt to the demands imposed by the traffic state, with the satellite playing an eminent role throughout.

VI. CONCLUSION

In this paper, we have introduced BLASTER, a framework that operates in an integrated TN-NTN, and is able to manage UE association, regulate power, and allocate bandwidth between the terrestrial and non-terrestrial tiers of the network. Our proposal is to adapt the network behaviour according to the traffic demand, i.e. focus on energy saving during low-traffic hours and offer large throughput otherwise. Simulation results show that BLASTER can greatly improve the network, enhancing the mean throughput during high-traffic hours, and scaling down the power consumption during low-traffic hours. We also underline the crucial and evolving role that the NTN play in the success of our framework, emphasizing the decisive part they are poised to play in ensuring ubiquitous and sustainable mobile services in the coming years.

REFERENCES

- [1] Y. Xu *et al.*, “A survey on resource allocation for 5g heterogeneous networks: Current research, future trends, and challenges,” *IEEE Communications Surveys & Tutorials*, vol. 23, no. 2, pp. 668–695, 2021.
- [2] D. López-Pérez *et al.*, “A survey on 5g radio access network energy efficiency: Massive mimo, lean carrier design, sleep modes, and machine learning,” *IEEE Communications Surveys & Tutorials*, vol. 24, no. 1, pp. 653–697, 2022.
- [3] T. Ahmed *et al.*, “The digital divide in canada and the role of leo satellites in bridging the gap,” *IEEE Communications Magazine*, vol. 60, no. 6, pp. 24–30, 2022.
- [4] M. Giordani and M. Zorzi, “Non-terrestrial networks in the 6g era: Challenges and opportunities,” *IEEE Network*, vol. 35, no. 2, 2021.
- [5] M. Benzaghta *et al.*, “Uav communications in integrated terrestrial and non-terrestrial networks,” in *2022 IEEE Global Communications Conference (GLOBECOM)*, 2022, pp. 1–6.
- [6] H. Alam *et al.*, “Throughput and coverage trade-off in integrated terrestrial and non-terrestrial networks: An optimization framework,” in *2023 ICC Workshops*, 2023, pp. 1553–1558.
- [7] E. Oh, K. Son, and B. Krishnamachari, “Dynamic base station switching-on/off strategies for green cellular networks,” *IEEE transactions on wireless communications*, vol. 12, no. 5, pp. 2126–2136, 2013.
- [8] X. Chen *et al.*, “Energy-efficiency oriented traffic offloading in wireless networks: A brief survey and a learning approach for heterogeneous cellular networks,” *IEEE Journal on Selected Areas in Communications*, vol. 33, no. 4, pp. 627–640, 2015.
- [9] S. Kaiming *et al.*, “Flexible multiple base station association and activation for downlink heterogeneous networks,” *IEEE Signal Processing Letters*, vol. 24, no. 10, pp. 1498–1502, 2017.
- [10] 3GPP TSG RAN, “TR 38.811, Study on New Radio (NR) to support non-terrestrial networks,” *V15.4.0*, 2020.
- [11] N. Piovesan *et al.*, “Machine learning and analytical power consumption models for 5g base stations,” *IEEE Communications Magazine*, vol. 60, no. 10, pp. 56–62, 2022.
- [12] Y. Shi, J. Zhang, and K. Letaief, “Group sparse beamforming for green cloud-ran,” *Wireless Communications, IEEE Transactions on*, vol. 13, 2013.
- [13] N. Parikh and S. Boyd, “Proximal algorithms,” *Found. Trends Optim.*, vol. 1, no. 3, p. 127–239, 2014.
- [14] T. Chen *et al.*, “Network energy saving technologies for green wireless access networks,” *IEEE Wireless Communications*, vol. 18, no. 5, 2011.
- [15] 3GPP TSG RAN, “TR 36.942, Evolved Universal Terrestrial Radio Access (E-UTRA); Radio Frequency (RF) system scenarios,” *V10.2.0*, 2010.
- [16] —, “TR 38.821, Solutions for NR to support non-terrestrial networks (NTN),” *V16.1.0*, 2021.
- [17] —, “TR 36.763, Study on Narrow-Band Internet of Things (NB-IoT) / enhanced Machine Type Communication (eMTC) support for Non-Terrestrial Networks (NTN),” *V17.0.0*, 2021.
- [18] —, “TR 38.901, Study on channel model for frequencies from 0.5 to 100 GHz,” *V17.0.0*, 2022.
- [19] —, “TR 36.814, Evolved Universal Terrestrial Radio Access (E-UTRA); Further advancements for E-UTRA physical layer aspects,” *V9.2.0*, 2017.
- [20] —, “TR 36.931, Evolved Universal Terrestrial Radio Access (E-UTRA); Radio Frequency (RF) requirements for LTE Pico Node B,” *V17.0.0*, 2022.